

‘Retrospective Analysis of Various Ct Imaging Features of Gist and Their Correlation with Histopathology’

Rajoo Ramachandran, Nishanth Nagarajan, Venkatesh Bala Raghu Raji, Sheela Chinnappan, Neelakanta Rajeev Roy.

Department of Radiology and Imaging Sciences,
Sri Ramachandra Institute of Higher Education and Research,
Porur, Chennai 600 0116, India

ABSTRACT

Gastro-intestinal stromal tumors are the commonest mesenchymal tumors of the gastrointestinal tract with variable malignant potential. Its origin can be anywhere between esophagus and rectum along with a variety of growth patterns. Contrast enhanced CT study of the abdomen is the most common imaging modality used for GIST evaluation in tertiary care centers. Although histopathological examination of the tumour sample is the gold standard for differentiating benign GIST from malignant GIST, it is possible to arrive at a diagnosis with a reasonable accuracy using imaging features alone. We conducted a retrospective study in our tertiary care centre taking into consideration the statistically significant CT imaging features and we assessed if there were any positive or negative associations of those factors with the final HPE diagnoses of GIST benign or malignant.

Keywords: - Gastro-intestinal stromal tumor; GIST, Intestinal lesions, Gastric lesions, Abdominal mass lesions.

INTRODUCTION:

Gastro-intestinal stromal tumors are nowadays considered the most common mesenchymal tumors of the gastrointestinal tract (GIT). The term stromal tumors was originally used to denote smooth muscle neoplasms of the alimentary tract, as designated by Clark and Marck in 1983. Originating from the interstitial cells of Cajal, these tumors can have a variable potential for malignancy. After extensive research by various teams, the inciting factor for gastrointestinal stromal tumors was proved to be a gain of function mutation involving the proto-oncogene c-KIT (CD 117 - a tyrosine kinase growth factor receptor), by Hirota and colleagues in 1998 [2]. Adding onto this, during the same year, Kindblom and colleagues, proved the interstitial cells of Cajal to be the cells of origin [3]. Thus, gastrointestinal stromal tumors were considered a distinct entity, separate from leiomyomas, leiomyosarcomas, nerve sheath tumors. GISTs can have three patterns on histological analysis - predominantly spindle cells (most common), predominantly epithelioid and mixed. However, Immunohistochemistry for CD117 (KIT) is considered the gold standard for diagnosing GIST. Contrast-enhanced computed tomography is the most common imaging modality used for evaluation of this entity and plays a pivotal role in imaging GISTs - both for diagnosis and follow-up. The mainstay of treatment includes surgical resection. This may or may not be followed by a course of chemotherapy - Imatinib mesylate.

MATERIALS AND METHODS:

This observational retrospective study was done between July 2017-2021 for a period of 4 years using 41 participants who underwent abdominal CECT imaging at department of Radiology in a tertiary care centre in Chennai, Tamil Nadu. Of the patients who had undergone contrast-enhanced computed tomographic examinations of the abdomen during this period, those patients diagnosed with gastrointestinal stromal tumor were taken up and studied extensively. The CECT examination was performed using GE Light Speed 64 slice VCT, operated at 90-120kV and 300 mAs. Plain sections were acquired, followed by non-ionic, iodine based contrast injection by Smart prep technique. The arterial phase images were acquired at 18-20 sec and venous phase at 40-60 sec. The radiological findings were correlated with histopathological results.

STATISTICAL METHODS:

Data collection was done using standard formats and entry was done with the help of Microsoft Office Excel. Data analysis was done using SPSS (Statistical Package for Social Sciences, IBM) version 16. Discrete variables were expressed as frequency and percentage while continuous variables were expressed as mean and standard deviation. Statistical association was established employing student t-test and chi square tests with a p value of < 0.05 within 95% confidence interval limits being considered statistically significant. ROC curve (fig. 1) was constructed for tumor size in the longest dimension and cut off values with optimal sensitivity and specificity was taken into consideration.

RESULTS:

This retrospective study was approved by the Institutional Ethics Committee. We studied 41 cases of histopathologically proven GIST in our tertiary care institute. We observed that males overall had a higher incidence of high-grade tumors than females. In the age group between ages 30 and 40, there was an equal incidence of high and low-grade tumors (2 each). As the age increases, the number of the high-grade tumors kept increasing than the latter, and the difference was striking in the age group between 60 and 70.

After a thorough review of the literature, we took into account the following critical imaging features to possibly predict the grade of the lesion with just the CT features. The statistics of various significance CECT imaging factors of GIST with their respective odds ratios and *p*-values (Table 1) as discussed below.

1. Site of lesion

We postulated that the primary location in itself contributes a significant risk of being a high-grade tumor. The majority of the lesions were seen from the stomach, and the next most common was the small bowel (duodenum > jejunum = ileum). Bowel lesions were common in high-grade (57.7%) and low-grade tumors (53.3%). With a *p*-value of 0.786, the site of lesion was considered statistically insignificant in our study. However, it is to be noted that 6 out of 7 (85.7%) arising from the duodenum proved to be of high grade.

2. Size:

The initial size of the tumor (longest diameter- LD) at the time of presentation played a role in the visual prognostication of the tumor. 80.8% of the tumors with size >10 cm have proven to be of high grade, with an odds ratio of 11.55 and p-value of 0.0014, which is statistically significant. 5 out of 6 tumors that measure less than 5 cm have proven to be of low grade, with an odds ratio of 0.08 and p-value of 0.03, which is statistically significant

A ROC curve was plotted using the longest dimension of the lesion, and a cut-off value of 10.0 cm was obtained (AUC – 0.796, p-0.02, C.I-0.635 – 0.957 and Sensitivity of 80.8% and Specificity of 72.3%).

3. Margins:

Lesion margin as a parameter in our study has proved to be a strong indicator of the malignant nature of the tumor. It has an odds ratio of 8.0 and a p-value of 0.021, which is statistically significant. 24 out of 33 (72.7%) tumors with ill-defined margins have been high-grade neoplasms.

4. Growth pattern

Growth patterns of the primary lesion in our study had different strengths of association and were not statistically significant. Three patterns of tumor growth have been described in the literature regarding GIST: endophytic, exophytic, and mixed. However, it is to be noted that none of the 4 cases with endophytic growth patterns turned out to be high grade whereas, the mixed pattern was observed with increasing frequency (38.5%) among the high-grade lesions.

5. Calcification

The presence of calcification was associated with 5.55 times the risk of the lesion being high grade with a statistical significance of 0.044. 12 out of 26 (46.2%) high-grade tumors had calcifications in the primary, while only 2 out of 15 (13.3) low-grade tumors exhibited them.

6. Necrosis

There is a consensus that high-grade lesions of any malignant neoplasm generally exhibit more necrosis than low-grade lesions, which was confirmed in our study for GIST. All 26 (100%) of the high-grade tumors exhibited necrosis of >50%. Necrosis of > 50% had an odd of 10.11 times the lesion being diagnosed as high grade with a statistical significance of 0.002.

7. Enhancement

The pattern of enhancement in GIST can be homogeneous or heterogeneous, and the latter is associated with a significantly higher probability of the tumor being high grade. In our study, only 3 cases showed homogeneous enhancement, and each one of them turned out to be of low grade, which was statistically significant [odds ratio of 0.067 and p-value of 0.0082]. A

heterogeneous enhancement pattern, on the other hand, showed no statistical significance and was observed in both 80% of low grade and 100% of high-grade lesions.

8. CT attenuation coefficient

In simple terms, the CT attenuation coefficient refers to the enhancement pattern of a tumor concerning the timing of the contrast administration. First, we calculate the relative values using which we calculate the absolute values. Our study calculated the relative CT attenuation coefficients of the tumors in the unenhanced, arterial, venous and delayed phases for all the samples by placing an equal-sized ROI in the solid portion of the tumor. The absolute enhancement CT attenuation coefficient value for each post-contrast phase was calculated by subtracting its relative CT attenuation coefficient from the unenhanced phase. We then deduced the phase in which the primary lesion showed an enhanced peak period based on these absolute enhancement CT attenuation coefficients.

The difference in the mean values of various parameters such as Hounsfield units for primary, arterial, venous and delayed parameters were statistically insignificant, implying that the difference is by chance and not an actual difference. When it comes to the enhancement pattern concerning the timing of the contrast administration, the majority of the high-grade tumors (24/26) exhibited maximum enhancement on the venous phase. A significant majority of the tumors that showed maximum enhancement in the delayed phase were low-grade tumors (5 out of 6 delayed enhancing tumors). We concluded that enhancement in the delayed phase is predominantly an attribute of low-grade tumors.

9. Metastases

Follow-up imaging was done with PET CT for 5 of our samples, with the interval varying between 6 months and one year. None of the low-grade tumors showed metastases in our study, while 6 out of the 26 (23.1%) high-grade tumors showed distant metastases. The presence of metastasis was associated with an odds ratio of 1.75 times (p-value of 0.04) of a high-grade lesion. GIST in our study metastasized to omentum, liver, and even to bone, which is considerably rare. Interestingly, the pathology of the case with bone metastases showed high-grade cell morphology with an increased mitotic rate (10/50).

10. Lymph nodes

Both high and low-grade lesions caused enlargement of the regional lymph nodes. 61.5% of the high-grade lesions and 73.3% of the low-grade lesions shows regional lymphadenopathy. No statistical significance could be established with lymph node as a parameter.

DISCUSSION:

INCIDENCE - Accounting for about 20 % of soft tissue sarcomas, on an average, gastrointestinal stromal tumors have an annual incidence of 10 per million population [1]. This however does not include ‘micro-GISTS’ - lesions smaller than a centimetre in diameter, which are found on histopathological examinations.

COMMON LOCATION-They can occur anywhere along the GI tract, mesentery, omentum, with stomach and jejunum being the most common sites. The large bowel and rectum are involved in around 5% of cases. Leiomyomas predominate in the esophagus. It has a wide age-group of incidence, with most prevalence between the sixth and seventh decades of life.

CLINICAL PRESENTATION-The presentation can be non-specific, varying depending upon the site of origin. Some of these include vague abdominal pain, bloating, abdominal mass, weight loss, ileus, gastrointestinal bleeding - in cases with mucosal involvement and rarely, intussusception. However, some of the GISTs may remain asymptomatic until upto the later stage, due to their location in the submucosa and its non-invasive nature. Pediatric GIST is a distinct entity, with a female preponderance, absence of KIT mutations, multicentric location in the stomach and a tendency for lymph nodal metastases [4].

SYNDROMIC GIST:

Few of the syndromes associated with GIST include:

- Type I neurofibromatosis - multiple GISTs, mostly multicentric in location, involving the small bowel [5].
- Carney triad syndrome - consisting of gastric GISTs, pulmonary chondromas and paragangliomas [6].
- Carney-Strarakis syndrome- consisting of GISTs and paragangliomas, secondary to mutations involving the subsets of succinate dehydrogenase [7].

IMAGING- Imaging helps in locating the primary tumor, staging of the disease and in assessment of treatment response. Useful modalities include Endoscopy, Endoscopic ultrasound (EUS), Computed tomography (CT), Magnetic Resonance Imaging (MRI) and Positron Emission Tomography (PET). The universal availability, standardised imaging protocols, assessment of disease beyond the primary site and multi-planar reconstruction/reformatting make contrast-enhanced CT - the imaging modality of choice at present [8] and play a mainstay in staging and monitoring treatment response. However, for rectal GISTs, MRI provides a better picture in the pre-operative assessment and staging [8].

The findings on CT may vary depending upon the tumor location, size and local invasion. They commonly present as a solitary mass, isodense to the muscle on non-enhanced images, with smooth margins. Being a highly vascular tumor, significant enhancement can be appreciated on post-contrast images.

Although a uniform consensus is not available, based on certain studies [9], benign GISTs generally tend to be smaller in size (gastric GISTs < or equal to 5 cm; intestinal GISTs < or equal to 2 cm) and show intense homogeneous enhancement following contrast administration. They are likely to present as either endoluminal, polypoidal or intramural masses.

On the other hand, malignant GISTs are larger in size (gastric GISTs >10 cm; intestinal GISTs >5 cm), with lobulated margins and an exophytic growth pattern. Heterogeneous enhancement is seen post-contrast, due to areas of hemorrhage, necrosis or myxohyaline degeneration [10]. This leads to a central hypodensity and the surrounding viable soft tissue produces a peripheral contrast enhancement.

Calcifications and ulceration of the tumor can also occur. The distribution of intralesional calcifications can be circumscribed and patchy. This likely occurs secondary to prior bleeding or necrosis of the tumor with cystic degeneration [11].

Mesenteric fat infiltration and invasion to adjacent structures are additional signs of malignancy. Other complications include fistula formation with adjacent structures [12] and rarely, bowel obstruction.

In a study by Tateishi et. al, it has reported that tumors larger than 11.1 cm, with an irregular surface/ unclear boundary, heterogeneous enhancement pattern, invasion to adjacent structures and presence of hepatic/ peritoneal metastases are more in favor of a high-grade gastro-intestinal stromal tumor. This has been shown to be associated with a reduced survival rate and a poorer prognosis [13].

In our study, we have observed that the following imaging factors have significant positive association in a lesion being malignant:

- o Longest diameter of the lesion greater than 10 cm
- o Ill-defined margins
- o High-grade necrosis (>50%)
- o Presence of calcification
- o Presence of metastases

The following imaging factors have significant negative association in a lesion being malignant:

- o Longest diameter of the lesion lesser than 5 cm
- o Homogeneous enhancement of the lesion

CONCLUSION:

Gastro-intestinal stromal tumors remain the most common mesenchymal tumors of all sections of the GI tract, with the exceptions of the esophagus, colon, and rectum, where leiomyomas are more common. Whilst histopathology remains the gold standard method to diagnose whether GIST in any given patient is benign or malignant, our research has proved that it is possible using imaging techniques to arrive at a diagnosis with reasonably accuracy. Using contrast-enhanced computed tomography we have analysed 10 important imaging factors of GIST, of which 5 have statistically significant positive and 2 have statistically significant associations with GIST being malignant. Using the longest dimension of the tumour, a cut off value of 10.0 cm was found to have optimal sensitivity and specificity in differentiating benign and malignant GIST.

REFERENCES:

1. Joensuu H, Hohenberger P, Corless CL. Gastrointestinal stromal tumour. *Lancet*. 2013 Sep 14;382(9896):973-83.
2. Hirota S, Isozaki K, Moriyama Y, et al. Gain-of-function mutations of c-kit in human gastrointestinal stromal tumors. *Science* 1998;279:577-80.
3. Kindblom LG, Remotti HE, Aldenborg F, et al. Gastrointestinal pacemaker cell tumor (GIPACT): gastrointestinal stromal tumors show phenotypic characteristics of the interstitial cells of Cajal. *Am J Pathol* 1998;152:1259-69.
4. Pappo, A.S. and Janeway, K.A. Pediatric gastrointestinal stromal tumors. *Hematol Oncol Clin North Am*. 2009; 23: 15–34
5. Miettinen, M., Fetsch, J.F., Sobin, L.H., and Lasota, J. Gastrointestinal stromal tumors in patients with neurofibromatosis 1: a clinicopathologic and molecular genetic study of 45 cases. *Am J Surg Pathol*. 2006; 30: 90–96
6. Zhang, L., Smyrk, T.C., Young, W.F. Jr et al. Gastric stromal tumors in Carney triad are different clinically, pathologically, and behaviorally from sporadic gastric gastrointestinal stromal tumors: findings in 104 cases. *Am J Surg Pathol*. 2010; 34: 53–64
7. Gaal, J., Stratakis, C.A., Carney, J.A. et al. SDHB immunohistochemistry: a useful tool in the diagnosis of Carney-Stratakis and Carney triad gastrointestinal stromal tumors. *Mod Pathol*. 2011; 24: 147–151
8. ESMO/European Sarcoma Network Working Group. Gastrointestinal stromal tumours: ESMO Clinical Practice Guidelines for diagnosis, treatment and follow-up. *Ann Oncol*. 2014 Sep;25 Suppl 3:iii21-6.
9. Miettinen M, El-Rifai WHL, Sobin L, et al. Evaluation of malignancy and prognosis of gastrointestinal stromal tumours: a review. *Hum Pathol*. 2002;33:478–483.
10. Sandrasegaran K, Rajesh A, Rushing DA, et al. Gastrointestinal stromal tumors: CT and MRI findings. *EurRadiol*. 2005;15:1407–14.
11. Ghanem N, Altehoefer C, Furtwangler A, et al. Computed tomography in gastrointestinal stromal tumors. *EurRadiol*. 2003;13:1669–78.
12. Burkill GJ, Badran M, Al-Muderis O, et al. Malignant gastrointestinal stromal tumor: distribution, imaging features, and pattern of metastatic spread. *Radiology* 2003;226:527–532.
13. Tateishi U, Hasegawa T, Satake M, et al. Gastrointestinal stromal tumor. Correlation of computed tomography findings with tumor grade and mortality. *J Comput Assist Tomogr*. 2003;27:792–798.

FIGURE LEGENDS:

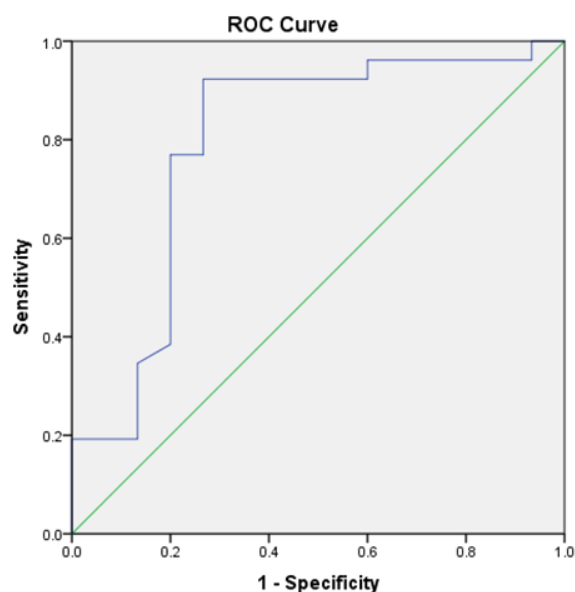


Figure 1: A Receiver Operating Characteristic (ROC) curve was constructed for tumor size in the longest dimension and cut off values with optimal sensitivity and specificity was taken into consideration. A cut off value of 10.0 cm was obtained (AUC – 0.796, $p=0.002$, C.I- 0.635 – 0.957) with a sensitivity of 80.8% and specificity of 72.3%, which qualifies as a screening test.



Figure 2 (a & b): 51-year-old case with malignant gastric GIST. Axial (a) and coronal (b) views of contrast-enhanced CT study of abdomen in venous show a lobulated enhancing soft tissue density mass lesion (solid arrow) at the gastric fundus in close proximity to gastro-esophageal junction. Few specks of calcifications (dashed arrow in b) are seen in the coronal view.

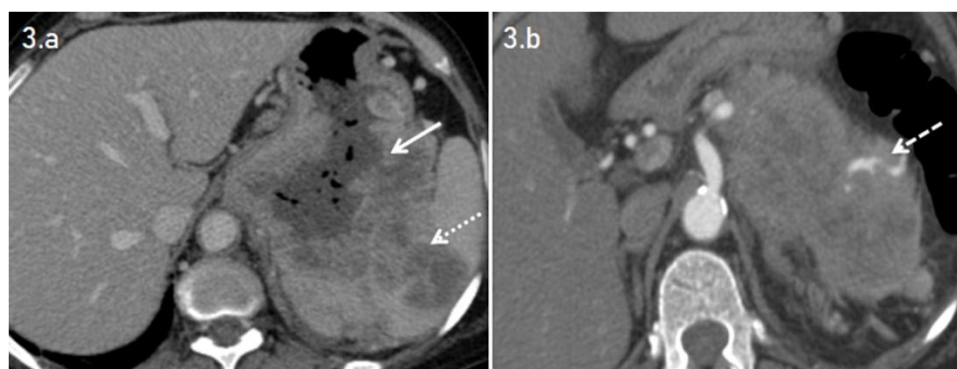


Figure 3 (a & b): 63-year-old case with malignant gastric GIST. Axial views of contrast-enhanced CT study of abdomen in venous (a) and arterial (b) phases show an exophytic, heterogeneously enhancing mass lesion (solid arrow) with central necrosis seen arising from the fundus of the stomach. The lesion is seen to infiltrate the splenic hilum (dotted arrow) with one third of the splenic parenchyma being replaced by the mass lesion. A prominent arterial feeder (dashed arrow in b) is seen arising from the splenic artery.

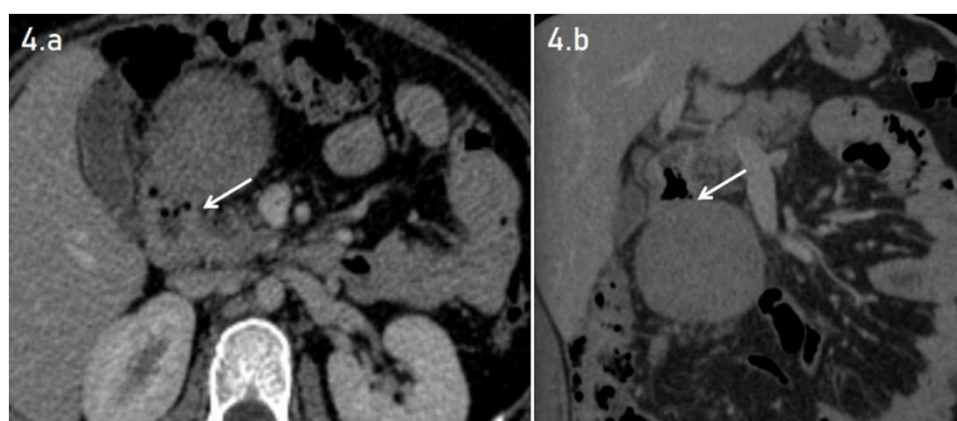


Figure 4 (a & b): 37-year-old case with benign duodenal GIST. Axial (a) and coronal (b) views of contrast-enhanced CT study of abdomen in venous show a well-defined ovoid soft tissue density lesion (solid arrow) arising from the second and third parts of the duodenum. The lesion is seen to arise exophytically without causing any upstream bowel dilatation.

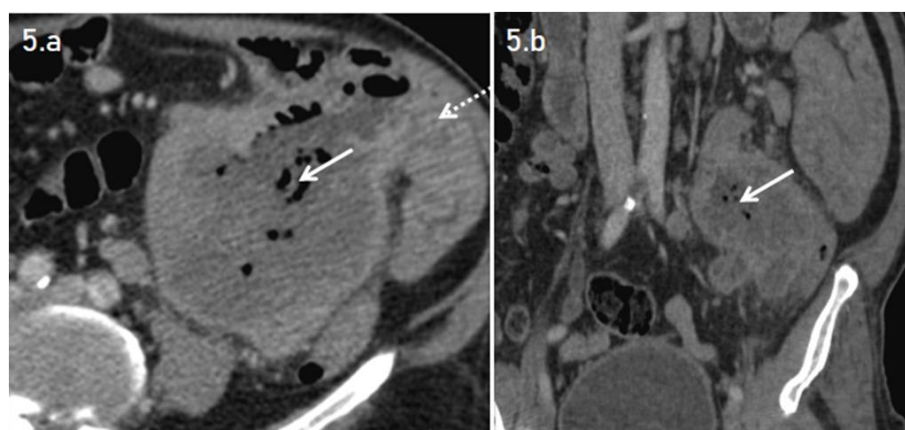


Figure 5 (a & b): 63-year-old case with malignant jejunal GIST Axial (a) and coronal (b) views of contrast-enhanced CT study of abdomen in venous show a large heterogeneous mass

with central necrosis (solid arrow) arising from the jejunum with loss of fat plane with the distal descending colon (dotted arrow).

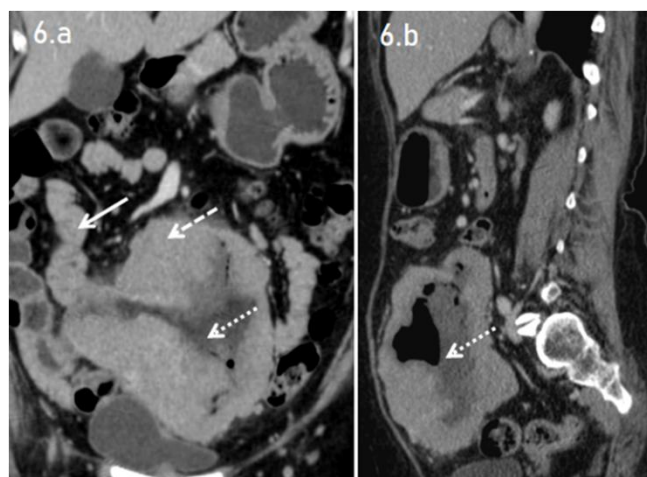


Figure 6 (a & b): 55-year-old case with malignant ileal GIST. Coronal (a) and sagittal (b) views of contrast-enhanced CT study of abdomen in venous show a large circumferential heterogeneously enhancing cavitating mass lesion (dashed arrow) arising from the ileum (solid arrow). The lesion shows central necrosis with air-fluid level (dotted arrow), indicative of the Torricelli-Bernoulli sign. The necrotic cavity is seen communicating with the lumen of the bowel.

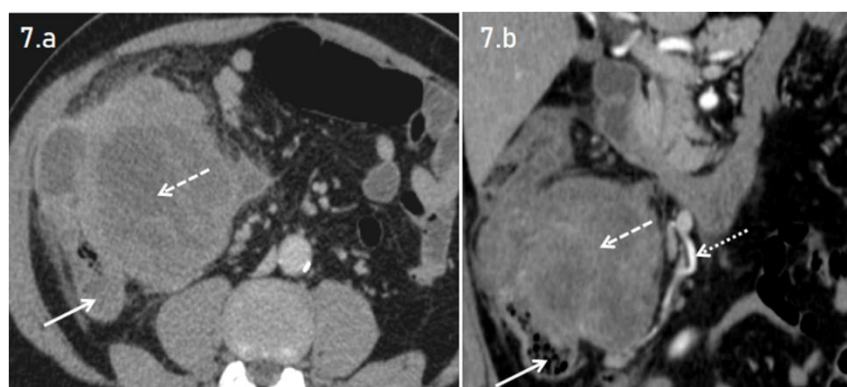


Figure 7 (a & b): 61-year-old case with malignant colonic GIST. Axial (a) and coronal (b) views of contrast-enhanced CT study of abdomen in venous show a large, exophytic heterogeneously enhancing lesion with central necrosis (dashed arrow) is seen arising from the medial wall of ascending colon (solid arrow). The lesion is seen compressing the ascending colon causing severe luminal narrowing. A prominent arterial feeder (dotted arrow in b) is seen arising from the superior mesenteric artery.

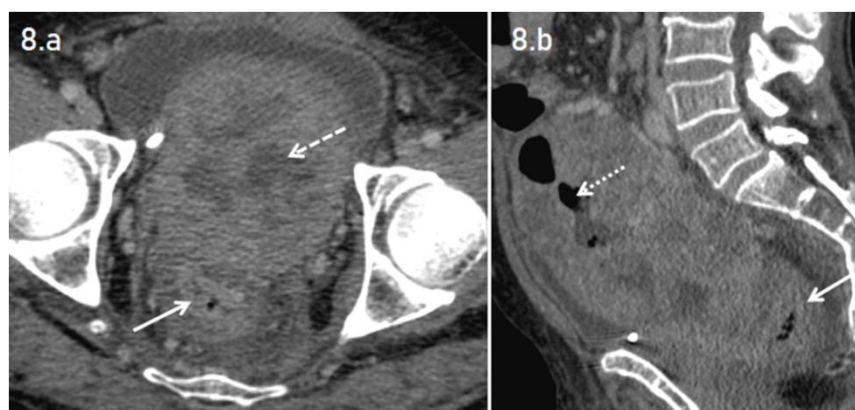


Figure 8 (a & b): 59-year-old case with malignant rectosigmoid GIST. Axial and sagittal views (a and b) of contrast-enhanced CT study of abdomen in venous phase show a large, well-defined, heterogeneously enhancing, exophytic soft tissue mass lesion with central non-enhancing necrotic areas (dashed arrow) and multiple air pockets (dotted arrow) arising from the rectosigmoid junction (solid arrow).

TABLE LEGEND:

Table – 1:

Parameter	High Grade	Low Grade	Odds Ratio	p value
Age				
< 50 years	17 (56.3)	8(43.8)	1.653	0.446
> 50 years	9 (63.4)	7(36.6)		
Site of lesion				
Stomach	11 (61.1)	7 (38.9)	0.838	0.786
Bowel	15 (65.2)	8 (34.8)		
Size				
< 5 cms	1 (3.8)	5 (33.3)	0.08	0.03
> 5 cms	25 (96.2)	10 (66.7)		
5-10 cms	4 (15.4)	6 (40.0)	0.273	0.086
Others	22 (84.6)	9 (60.0)		
> 10 cms	21 (80.8)	4 (26.7)	11.55	0.0014
< 10 cms	5 (19.2)	11 (73.3)		
Margins				
Ill defined	24 (72.7)	9 (27.3)	8.00	0.021
Well defined	2 (25.0)	6 (75.0)		
Growth pattern				
Exophytic	16 (61.5)	9 (60.0)	1.066	0.922
Others	10 (38.5)	6 (40.0)		
Endophytic	0 (0.0)	4 (26.7)	0.048	0.0478
Others	26 (100.0)	11 (73.3)		
Combined pattern	10 (38.5)	2 (13.3)	4.061	0.103
Others	16 (61.5)	13 (86.7)		
Calcification				
Present	12 (46.2)	2 (13.3)	5.57	0.044
Absent	14 (53.8)	13 (86.7)		

Necrosis				
< 50%	26 (100.0)	4 (26.7)	<u>10.01</u>	<u>0.002</u>
> 50%	0	8 (73.3)		
Enhancement				
Homogenous	0 (0.0)	3 (20.0)	<u>0.067</u>	<u>0.0082</u>
Heterogenous	26 (100.0)	12 (80.0)		
Metastasis				
Present	6 (23.1)	0 (0)	<u>1.75</u>	<u>0.044</u>
Absent	20 (76.9)	15 (100.0)		
Lymph Nodes				
Present	16 (61.5)	11 (73.3)		
Absent	10 (39.5)	4 (26.7)	1.71	0.445

Table 1: shows the statistics of various significance CECT imaging factors of GIST with their respective odds ratios and *p*-values.